Since January 2020 Elsevier has created a COVID-19 resource centre with free information in English and Mandarin on the novel coronavirus COVID-19. The COVID-19 resource centre is hosted on Elsevier Connect, the company's public news and information website.

Microporous and Mesoporous Materials 334 (2022) 111760

Contents lists available at ScienceDirect

Microporous and Mesoporous Materials

journal homepage: www.elsevier.com/locate/micromeso

Modification of face masks with zeolite imidazolate framework-8: A tool for hindering the spread of COVID-19 infection

Daria Givirovskaia [a,*], Georgy Givirovskiy [a], Marjo Haapakoski [b], Sanna Hokkanen [a], Vesa Ruuskanen [a], Satu Salo [c], Varpu Marjomäki [b], Jero Ahola [a], Eveliina Repo [a]

[a] LUT University, P.O. Box 20, FI-53851, Lappeenranta, Finland
[b] University of Jyväskylä, P.O. Box 35, FI-40014, Jyväskylä, Finland
[c] VTT Technical Research Centre of Finland Ltd., P.O. Box 1000, FI-02044, ESPOO, Finland

ARTICLE INFO

Keywords:
MOFs
ZIF-8
COVID-19 pandemic
Face masks
Anti-viral/bacterial coating

ABSTRACT

The worldwide spread of the SARS-CoV-2 virus has continued to accelerate, putting a considerable burden on public health, safety, and the global economy. Taking into consideration that the main route of virus transmission is via respiratory particles, the face mask represents a simple and efficient barrier between potentially infected and healthy individuals, thus reducing transmissibility per contact by reducing transmission of infected respiratory particles. However, long-term usage of a face mask leads to the accumulation of significant amounts of different pathogens and viruses onto the surface of the mask and can result in dangerous bacterial and viral co-infections. Zeolite imidazolate framework-8 (ZIF-8) has recently emerged as an efficient water-stable photocatalyst capable of generating reactive oxygen species under light irradiation destroying dangerous microbial pathogens. The present study investigates the potential of using ZIF-8 as a coating for face masks to prevent the adherence of microbial/viral entities. The results show that after 2 h of UV irradiation, a polypropylene mask coated with ZIF-8 nanostructures is capable of eliminating *S. Aureus* and bacteriophage MS2 with 99.99% and 95.4% efficiencies, respectively. Furthermore, low-pathogenic HCoV-OC43 coronavirus was eliminated by a ZIF-8-modified mask with 100% efficiency already after 1 h of UV irradiation. As bacteriophage MS2 and HCoV-OC43 coronavirus are commonly used surrogates of the SARS-CoV-2 virus, the revealed antiviral properties of ZIF-8 can represent an important step in designing efficient protective equipment for controlling and fighting the current COVID-19 pandemic.

1. Introduction

Millions of people worldwide have suffered from COVID-19, which is caused by the novel SARS-CoV-2 virus, many of whom have died [1]. It is believed that a primary route of COVID-19 transmission is via the respiratory particles, and all infected individuals, regardless of the course of the disease, are considered possible transmitters and thus represent a threat [2]. Various measures, including mass vaccination programs, city-wide lockdowns, travel restrictions, and hygiene and social distancing guidelines have been imposed in many countries as a part of efforts to stop, or at least limit, the transmission of COVID-19 [3]. Following interim guidance published by the World Health Organization (WHO) in 2020, the use of protective face masks in public places has become increasingly recommended, if not mandated, to prevent the spread of the disease [4]. In the review published by Howard et al. [2], an analytical framework was used to provide evidence that widespread mask usage is the most efficient way of reducing the spread of COVID-19 if compliance is high. In a different study performed by Liang et al. [5], meta-analysis revealed that a significant protective effect can be achieved by using a face mask as the risk of respiratory virus infection can be reduced by 80% and 47% for healthcare workers (HCWs) and non-healthcare workers (non-HCWs), respectively. The systematic review by Jefferson et al. [6] also shows that simple public health measures including hand-washing, isolation of potentially infected patients, and wearing of masks are effective in preventing the spread of respiratory virus infections. As a result, huge public demand for face masks has developed, manufacture and supply have been under strain, and deficits have been reported in many countries, leading to the imposition of measures enhancing production capacities while prohibiting the export of face masks [7]. Enormous demand and a shortfall in face mask availability has motivated a search for new solutions, such as disinfection of used masks, reuse of masks initially developed as one-use disposable masks, and fabrication of non-certified homemade masks [8].

* Corresponding author.
E-mail address: daria.givirovskaia@lut.fi (D. Givirovskaia).

https://doi.org/10.1016/j.micromeso.2022.111760
Received 23 December 2021; Received in revised form 8 February 2022; Accepted 9 February 2022
Available online 21 February 2022

Despite research like the aforementioned indicating the positive effect of wearing masks on the current pandemic, understanding of the influence of masks on the transmission of laboratory-diagnosed respiratory viruses remains incomplete [9–11]. For example, research on mask effectiveness [12] does not take into consideration that bacteria in human saliva and exhaled breath might constitute a biosafety concern [13], particularly with long-term mask usage or mask reuse without appropriate disinfection. Hasan et al. [14] investigated the bacterial flora of saliva microbiomes using next-generation shotgun sequencing (NGSS) and identified more than 175 different bacterial species, among which were life-threatening species of *Haemophilus influenzae, Neisseria meningitidis*, and *Streptococcus pneumoniae*. It would appear that during breathing, sneezing or coughing by COVID-19-infected individuals, such airborne respiratory pathogens are trapped by the masks and accumulate on the surface layers of mask [15]. At the same time, moisture retention under the mask surface reduces the mask's protective properties and creates favorable conditions for bacterial growth [16]. In a recent study by Sharifipour et al. [17], the authors emphasized concerns that bacterial co-infections due to *Acinetobacter baumannii* and *Staphylococcus aureus* could be leading to superinfection of COVID-19 patients. Hence, bacterial co-infection and secondary bacterial infection should be considered critical risk factors influencing the severity and mortality rates of COVID-19 [18].

In recent years, a number of different nanomaterials, such as Ag [16,19], Cu [20,21], Zn [22], Ti [23] and Au [24] nanoparticles, have been developed to enhance the anti-viral and anti-bacterial properties of materials, which opens new perspectives in the prevention of COVID-19 transmission [25]. Within this context of nanomaterial development, metal–organic frameworks (MOFs) have attracted huge scientific interest as a fast-developing field of research with an increasing number of applications being proposed [26–42]. MOFs are organic–inorganic hybrid crystalline porous materials with unique properties including: (i) exceptional surface area extending beyond 6000 $m^2 g^{-1}$, (ii) ultrahigh porosity of up to 90% of free volume, (iii) structural diversity in contrast to other porous materials, and (iv) controllable framework topology, porosity, and functionality [43]. In view of these advantageous properties, MOF-based antibacterial agents are gaining increasing importance [44]. Compared to traditional antibacterial agents, MOFs provide several important advantages, such as (i) the presence of bactericidal metal ions, (ii) a chelation effect increasing lipophilicity and facilitating penetration to the bacterial cell to destroy it, (iii) the ability to form photogenerated reactive oxygen species (ROS) enhancing photocatalytic antimicrobial effects, (iv) the possibility of achieving synergistic antimicrobial effects in a single MOF structure, for example, a combination of photocatalytic and metal ion-releasing effects, and (v) the possibility of encapsulating various materials in the pores of the MOFs [44].

Zeolitic imidazolate frameworks (ZIFs) are a subclass of MOFs presented by porous crystals with zeolite-type structures built by metal ions and imidazolate ligands [45]. Among different MOFs, ZIF-8 (zinc-imidazolate MOF) has been highlighted as an efficient water-stable antimicrobial photocatalyst exhibiting >99.9999% inactivation efficiency against *Escherichia coli (E. coli)* and outperforming reference ZnO and TiO_2 biocidal photocatalysts [46]. The high antimicrobial efficiency of ZIF-8 is due to a complicated mechanism involving the capture of photoelectrons by Zn^+ centers via ligand-to-metal charge transfer (LMCT) and subsequent O_2-reduction-based generation of ROS capable of inhibiting pathogens. In view of the beneficial photocatalytic properties of ZIF-8, this research examines ways of using ZIF-8 as an antiviral/antibacterial coating for the surfaces of commercial face masks (Fig. 1). Additionally, the work analyzes the efficiency of ZIF-8-based coating against dangerous microbial pathogens and SARS-CoV-2's surrogates which provides fresh insights into the field and to already successfully developed solutions [47–49]. The research contributes to the global response to addressing COVID-19 by examining a potentially effective solution for reusable protective materials capable of deactivating SARS-CoV-2 virus and other respiratory viruses [50–52].

2. Materials and methods

2.1. Materials

All chemical reagents used for the experimental work were from Sigma-Aldrich, USA, and used without pretreatment (if not otherwise stated). Polypropylene (PP) masks for MOFs growing were purchased from KINGFA, China, and Teho Filter, Finland. The Hele cloth mask (49% polyester, 49% cotton, 2% elastane) was supplied by Helemed, Finland. The LUT-branded cloth mask (100% polyester) was designed by LUT-University, Finland, and manufactured by LS-Wear, Finland.

2.2. Modification of the face masks with ZIF-8

The procedure for the ZIF-8 synthesis was adapted from previous research [46,53]. A schematic representation of the coating experiments is shown in Fig. 2.

Method A: Room temperature synthesis was performed in a glass vessel under magnetic stirring. First, 0.3 g of terephthalic acid was added to 30 mL dimethylformamide (DMF) and left under magnetic stirring for 30 min. Subsequently, 0.25 g of zinc acetate dihydrate dissolved in 10 mL ethanol was added and the mixture was left under magnetic stirring for 24 h. After mixing, the solution was pipetted directly onto the polypropylene (PP) fabric, which was then wrapped in aluminum foil, and heated with an iron at a temperature of 110 °C for 2–3 min on both sides. The fabric was washed with water and dried in an oven at 80 °C for 30 min and then activated at 120 °C for 6 h.

Method B: Zinc acetate dihydrate, 2-methylimidazole, and polyethylene glycol were mixed in mass fractions of 15.9%, 39.7%, and 44.4%, respectively. Masks were split into layers if required, placed on the aluminum foil and the mixture was deposited onto the layers. The skin layer of the masks was not used for the growing procedure if the mask consisted of more than one layer. The masks were ironed at 110 °C for 1 min on both sides and washed with ethanol. Then the samples were dried at 80 °C for 30 min and activated for 6 h at 120 °C.

2.3. SEM and XRD characterization

A variable pressure scanning electron microscope (SEM) Hitachi S-3400N with X-ray spectroscopy (EDX) was applied for analysis of the ZIF-8 morphology on the mask surfaces. The microscope was operated at 20 mA and 10 kV with secondary (UDV) and backscatter (BSE) electron detectors. X-ray diffraction analysis (XRD) was performed with a Bruker D8 Advance X-ray diffractometer to examine the material crystal structure. Surface scanning was performed at a wavelength of 1.5406 Å with Cu Kα-type radiation produced by copper sealed tube X-ray source.

2.4. ZIF-8 coating stability tests

4 mask material samples of 4 × 4 cm were placed in a 300 mL vessel of boiling water for 15, 30, 45, and 60 min. Simultaneously, 2 mask samples of the same size were steamed in a water bath for 15 and 30 min. After the experiment, all the samples were dried and compared with the reference material using XRD analysis.

2.5. Selection of bacteria and viruses

Staphylococcus aureus (S. Aureus) (VTT E-70045), which is commonly used for measuring antimicrobial efficacy, was selected as a microbial pathogen. *S. Aureus* co-infection causes bacteraemia and pneumonia in patients infected with COVID-19 and is associated with a high mortality rate of 66.7% [54]. Bacteriophage MS2 (DSM 13767) is a surrogate for the influenza virus and is now being used as a surrogate for other RNA viruses, such as SARS CoV-1 and SARS CoV-2 [55]. Finally, low-pathogenic coronavirus (HCoV-OC43) was selected for the experimental work as it has certain genetic similarities with the SARS CoV-2 [56].

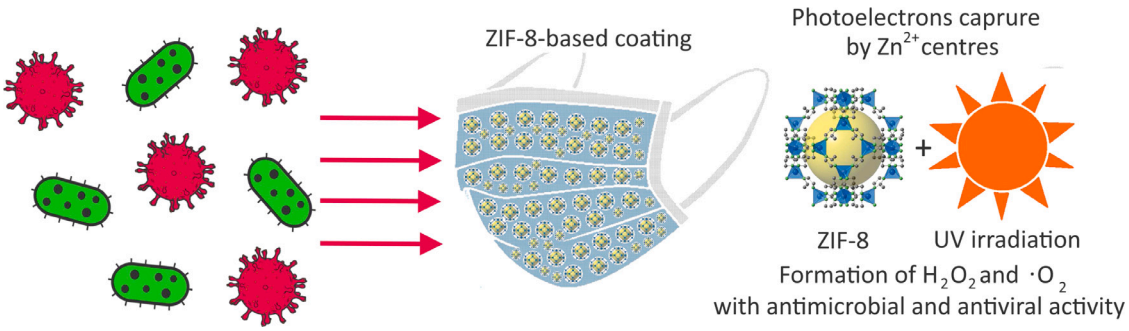

Fig. 1. Schematic representation of the ZIF-8-based mask antiviral and antibacterial mechanism.

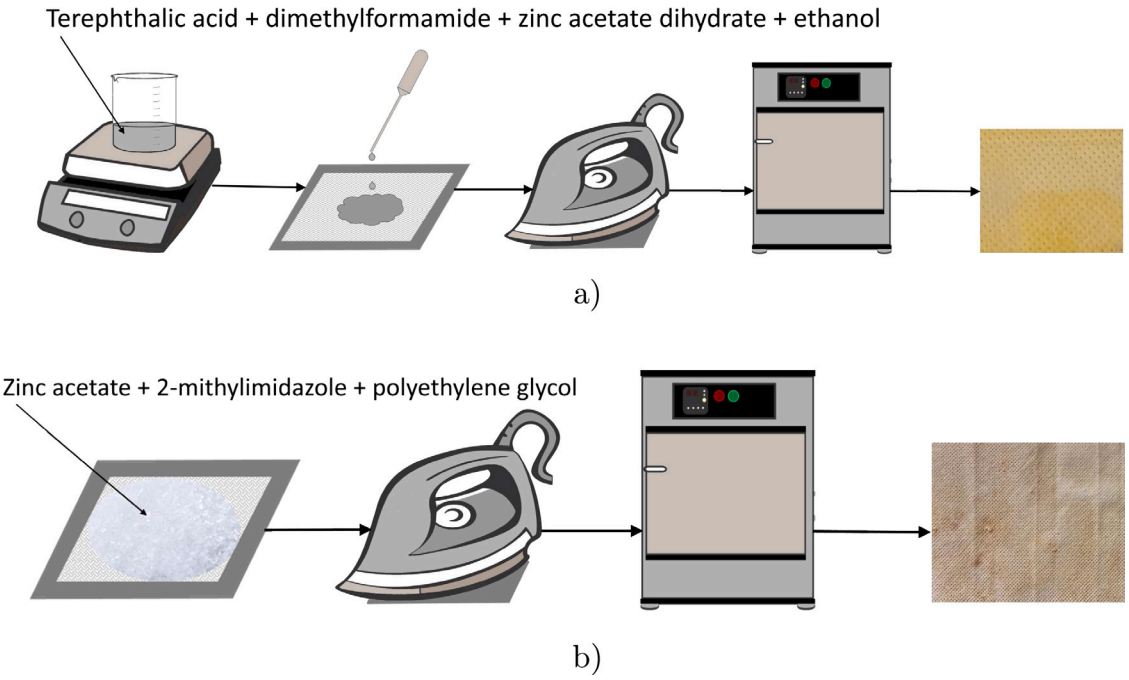

Fig. 2. Schematic representation of a modification of face masks with ZIF-8 photocatalyst using (a) Method A and (b) Method B.

2.6. Measurement of antibacterial activity

The antibacterial efficacy of the modified mask materials was studied based on the international standard ISO 22196:2011 "Measurement of antibacterial activity on plastics and other non-porous surfaces". The principle of the antibacterial efficacy tests is to bring the antibacterial surface and tested organisms into contact and detect surviving microbes after a specified contact time. Contamination of the tested surface was performed by dosing 0.4 mL of the microbe suspension onto 5 cm^2 of reference and ZIF-8-modified mask samples. Next, the contaminated surface was covered with a 4 cm^2 sterile plastic plate to prevent moisture evaporation and left for 2 h at room temperature. Subsequently, remaining microbes were diluted from the surface with 10 mL peptone saline solution, and the viability of the microbes was determined using culturing methods. The survival of microbes on the tested antibacterial surfaces was compared to a reference mask sample without ZIF-8-based coating. The photocatalytic activity of the MOF structures was studied by the same method, but the samples were under a UV lamp (365 nm) during contact time.

2.7. Antiviral tests with low-pathogenic coronavirus

The efficacy of the modified mask materials against HCoV-OC43 was studied based on the international standards EN 14476 "Quantitative suspension test for the evaluation of virucidal activity in the medical area" and EN 14885 "Chemical disinfectants and antiseptics" with certain modifications. In the antiviral tests, MRC-5 cells (1.5×10^4 cells/well) purchased from ATCC were seeded into 96-well plates in Minimum Essential Media (MEM, Gibco Life Technologies) supplemented with 10% Fetal Bovine Serum (Gibco), 1% GlutaMAX (Gibco) and 1% penicillin/streptomycin (Gibco) and incubated for 24 h at 37 °C (5% CO_2). The following day, 5 μL of seasonal human coronavirus HcoV-OC43 (1.6×10^7 pfu/mL) was placed on the surface of 1 cm^2 mask pieces for 1 h inside a 12-well plate at room temperature and in humid conditions. Incubation was performed with and without exposure to UV light (365 nm). The distance between the UV lamp and samples was 15 cm and the samples were covered with thin plastic foil. A culture medium (995 μL of 2% MEM) was added onto the surface of the mask pieces after the incubation period and placed on a rocker for 1 min to detach the virus. Media were then collected and diluted (1:100) samples were added onto MRC-5 cells in 96-well plates (MOI = 0.004). Cells were incubated for 5 days at 34 °C until a cytopathic effect (CPE) was observed. The cells were then washed twice with phosphate-buffered saline (PBS) solution, and stained with CPE stain (0.03% crystal violet, 2% ethanol, and 36.5% formaldehyde) for 10 min at room temperature. The excess stain was washed away with water. The stained cells were then treated with a lysis buffer (0.8979 g of sodium citrate and 1N HCl in 47.5% ethanol) to homogenize the sample. Finally, the absorbance of

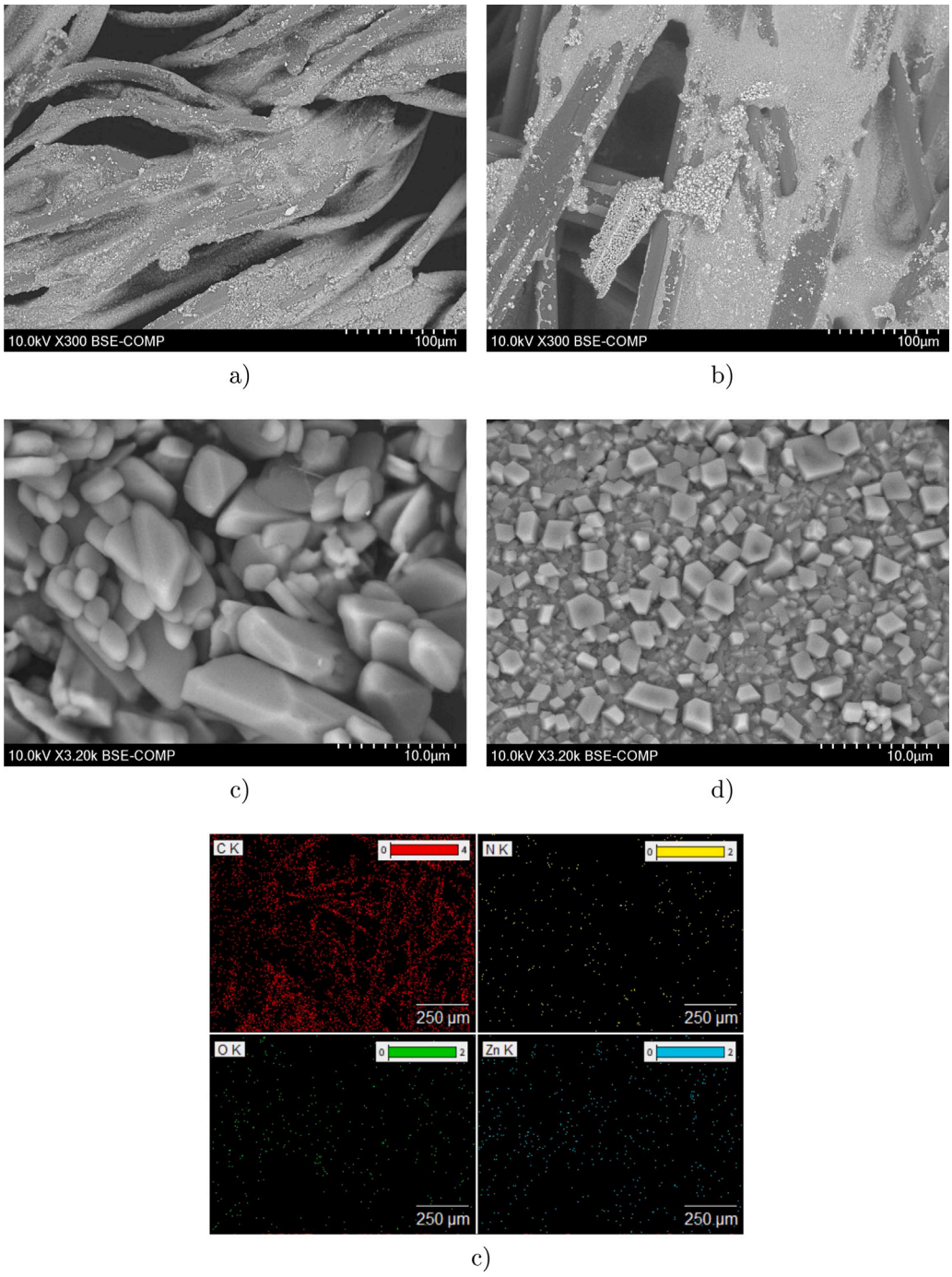

Fig. 3. SEM images of ZIF-8 deposited on (a) non-woven material (Teho Filter), and (b) woven material (LUT-branded cloth mask), morphology of ZIF-8 photocatalyst synthesized by (c) Method A, and (d) Method B, and (e) example of elemental mapping.

the stain was measured at 570 nm to determine the presence of viable cells in the wells, which indirectly shows the level of infection (Victor X4 2030 Multilabel Reader, PerkinElmer).

3. Results and discussion

3.1. Modification of face masks with ZIF-8

Different mask materials described previously were first tested as substrates for ZIF-8 deposition. Successful incorporation of nanocrystalline ZIF-8 onto the mask substrates was confirmed by SEM and EDX analysis. The obtained SEM images are presented in Fig. 3a and b and reveal a uniform coating of non-woven and woven mask samples with ZIF-8 micrometer/nanometer-size particles, indicating good suitability of both substrates for ZIF-8 deposition. As the substrate did not play a significant role in the quality of deposition, masks made of polypropylene, which is the material now recommended by the WHO for COVID-19 mask filters, were selected for further experiments. It is worth mentioning that the use of slightly different synthesis methods resulted in completely different surface morphologies. In the case of Method A synthesis (Fig. 3c), the ZIF-8-based coating is formed by hexagonal-shaped crystals and spheres as well as cubes with rounded edges. With Method B synthesis (Fig. 3d), on the other hand, the ZIF-8 layer on the surface of the mask substrates is mostly formed of numerous rhombic dodecahedron particles. The SEM images show that most

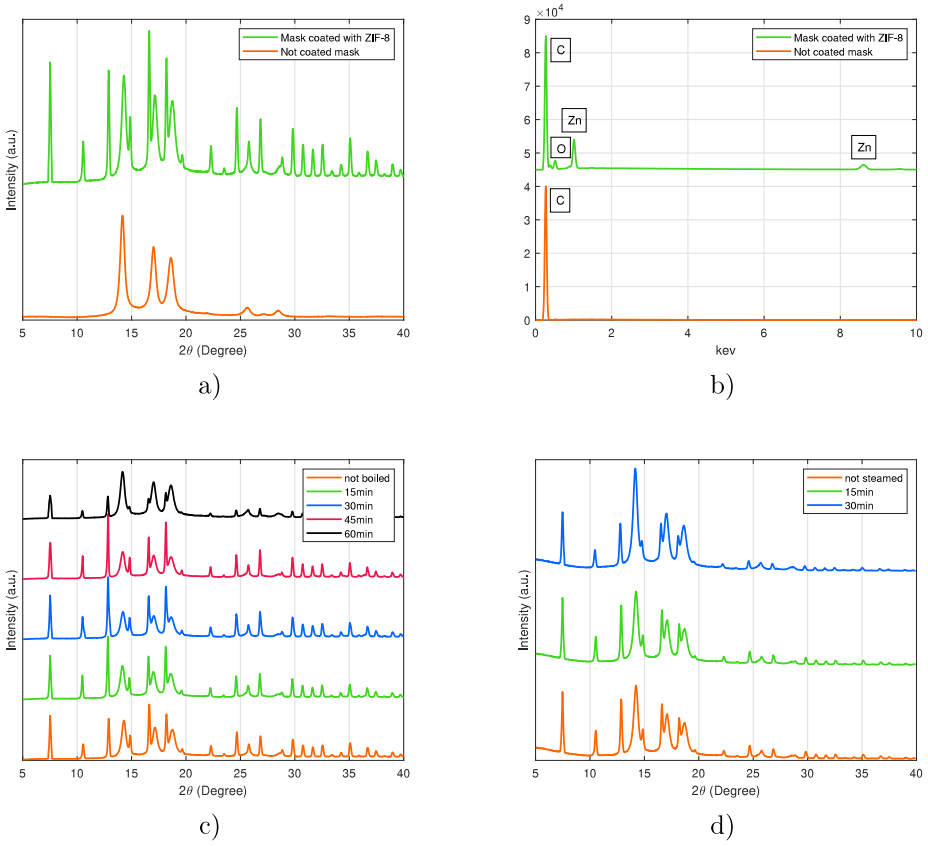

Fig. 4. Comparison of ZIF-8-modified and uncoated mask materials by (a) XRD analysis and (b) EDX analysis, and recorded XRD patterns after chemical stability tests by (c) boiling, and (d) steaming.

of the crystals have good uniformity, sharp edges, and well-defined facets when using Method B for the photocatalyst preparation. Curiously, the sizes of the synthesized crystals vary considerably. Method A synthesis results in much larger ZIF-8 based crystals than Method B synthesis, and huge particles reaching 90–110 μm can be found on the mask material surface. The typical size of dodecahedron particles after Method B synthesis is in the range of 500–1000 nm. Even though the specific surface area and the pore volume of the synthesized particles using Method B were not measured in this study, according to the literature [57] and based on the size of particles the aforementioned parameters correspond to approximately $1500\,m^2\,g^{-1}$ and $0.55\,cm^3\,g^{-1}$, respectively. The difference in the size of the crystals is likely due to the difference in the temperature of the synthesis methods. In Method A synthesis, ZIF-8 was formed at room temperature during mixing while in Method B synthesis, the formation was performed in situ on the mask during ironing at 110 °C. In both cases, simultaneous coexistence of small and large crystals was observed, which can be explained by heterogeneous nucleation of crystals at the surface of existing crystals [58].

XRD patterns were recorded for the mask samples prior to and after coating with ZIF-8. A typical XRD diagram of the ZIF-8 photocatalyst deposited on the PP mask is presented in Fig. 4a. Characteristic diffraction peaks for ZIF-8 were observed at 7.4°, 10.4°, 12.7°, 14.7°, 16.4°, 18.0°, 22.1°, 24.5°, 26.7°, 29.6°. The diffraction peaks correspond well to crystallographic planes obtained from pure ZIF-8 nanocrystals [45,57], which confirms the inherent sodalite structure and high crystallinity of the synthesized particles. The relative intensity of some peaks differs from pure ZIF-8, presumably due to the change of preferred orientation of the nanocrystals growth on PP substrate, or affinity interactions between the ZIF-8 lattice and PP substrate. The chemical stability of the ZIF-8-modified masks was examined by suspending the masks in boiling water and applying steam to mimic typical sterilization processes. During this process, samples were periodically checked with XRD analysis, which revealed high stability of ZIF-8 coatings. Based on the XRD analysis, a minor change in peak intensity was only observed after 60 min of boiling, whereas no changes were observed with shorter boiling time, nor during the steam sterilization process.

3.2. Activity of ZIF-8-modified masks against S. aureus and MS2

First, the anti-bacterial/viral properties of ZIF-8-modified PP masks were examined by exposing mask samples to *S. Aureus* and MS2 bacteriophage for 2 h. From the results presented in Fig. 5, it can be seen that mask material modified with ZIF-8 using Method A showed low activity against *S. Aureus* and MS2 Bacteriophage comparable to a reference PP mask without coating. The PP mask coated with ZIF-8 using Method B exhibited exceptionally high activity against both *S. Aureus* and the MS2 bacteriophage. After 2 h of experimental time under UV light, the inactivation efficacy against *S. Aureus* of Sample B reached 99.99%, which is equivalent to a 4 log reduction. This result is comparable with the efficiency reached by ZIF-8 in studies of Li et al. [46] against *E. Coli* and lower in comparison to sophisticated ZIF-8-based nanodagger arrays published in [59]. Curiously, Sample B showed good antibacterial properties against *S. Aureus* even without UV light irradiation, reaching inactivation efficacy of 99.95% corresponding to a 3 log reduction. The difference in the performance of the two samples became even more clear in the experiments with the MS2 bacteriophage. Sample A did not show any antiviral properties without UV irradiation whereas Sample B managed to reduce the amount of MS2 colonies by approximately 90%. Under UV irradiation, the reduction of MS2 reached 22% and

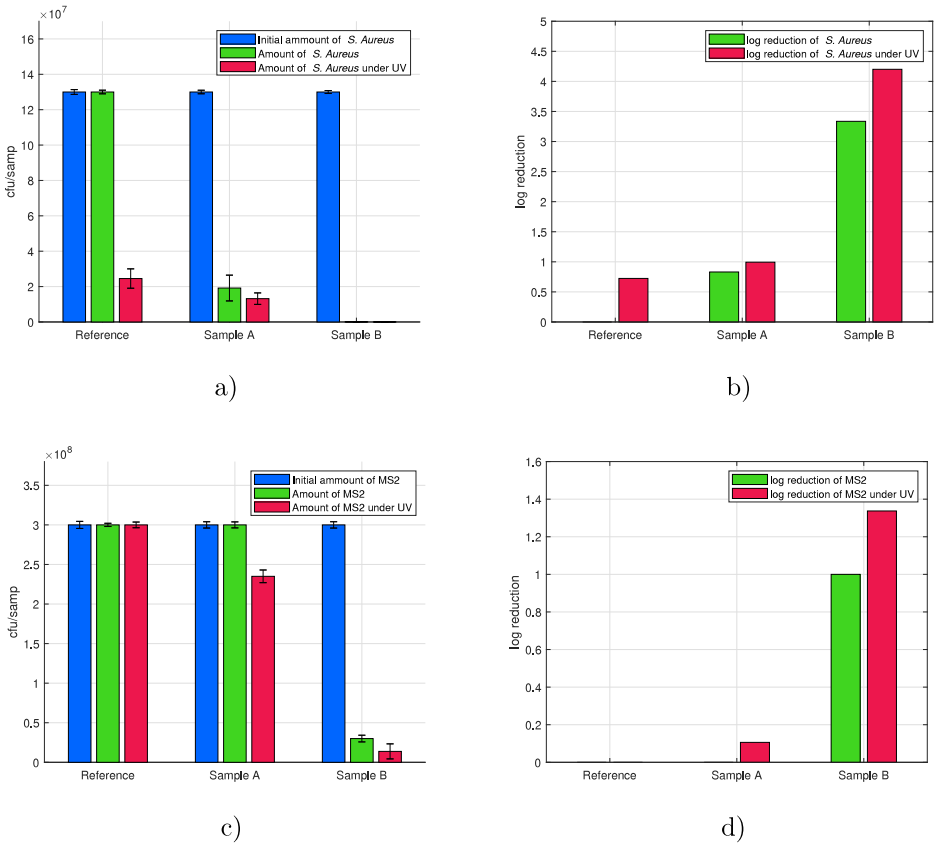

Fig. 5. Results of anti-bacterial/viral efficacy tests and corresponding log reduction after 2 h of contact time of ZIF-8-modified mask materials with (a–b) *S. Aureus* and (c–d) MS2 bacteriophage.

95.4%, respectively, for Samples A and B. Taking into account that both coatings are mainly composed of Zn, the different anti-bacterial/viral activities should be a direct consequence of the surface morphology, independent of the chemical composition.

3.3. Activity of ZIF-8-modified masks against HCoV-OC43

The results of antiviral activity tests against HCoV-OC43 achieved by cytopathic effect assay are presented in Fig. 6. It is worth mentioning that the number of living cells is presented as absorbance of A570. The virus control shows a low absorbance due to most of the cells killed left to stain for blue color. In contrast, the cell control without any virus infection shows the maximum cell viability, i.e. high absorbance. Importantly, high viability in Fig. 6b means that ZIF-8-based coatings are not toxic when tested in human cell cultures indicating safe use as a coating for commercial face masks. According to the results, PP mask material modified with ZIF-8 using Method B was showing high antiviral activity against HCoV-OC43 under UV irradiation. The infectivity of HCoV-OC43 was totally inhibited when the virus was exposed to UV light irradiation (365 nm) for 1 h on top of Sample B. At the same time, mask material modified with ZIF-8 using Method A exhibited moderate antiviral efficacy against the virus which can be once again explained due to differences in surface morphology. Surprisingly, Sample B showed a mild antiviral effect even without UV irradiation while there was absolutely no effect of Sample A at similar conditions. Taking into consideration that the uncoated reference sample did not show any antiviral activity with or without UV irradiation, the obtained results point to the antiviral properties of ZIF-8-based coatings. Evidently, the antiviral activity of both ZIF-8-based coatings, especially Sample B, is increased when exposed to UV light. Presumably, the ROS generated by the photoactivation of ZIF-8 lead to a breakage or damage of viral particles leading to inhibition of HCoV-OC43 infectivity. The ability of ROS to inactivate enveloped viruses, such as HIV has been previously documented [60] as well as the ability of H_2O_2 to inactivate rabies and influenza virus [61,62]. However, the exact mechanism in the case of HCoV-OC43 remains to be studied.

4. Conclusions

In the present study, different commercially available face masks were successfully modified with ZIF-8. All tested mask materials, which included both woven and non-woven samples, were shown to be good substrates for ZIF-8 deposition. However, a slight difference in the ZIF-8 synthesis procedures resulted in significant changes in particle size, which induced distinctive changes in anti-bacterial/viral performance. It was revealed that the PP mask coated with nanometer-size ZIF-8 particles exhibited high inactivation efficacy against *S. Aureus*, bacteriophage MS2, and low-pathogenic HCoV-OC43 coronavirus. Under UV irradiation, inactivation efficiency reached 99.99% and 95.4% after 2 h of contact time, respectively for *S. Aureus* and bacteriophage MS2, while in case of HCoV-OC43 coronavirus inactivation efficiency achieved 100% after 1 h of contact time. Even though the photocatalytic mechanism of ROS generation capable of inhibiting pathogens was previously known for ZIF-8 and MOF has previously been found to have good antibacterial properties, the present research highlights also the antiviral properties of ZIF-8 against surrogates of SARS-CoV-2. Furthermore, a valuable finding of this work demonstrates that developed ZIF-8-based coatings have negligible effects on human cells in the culture and thus, are not harmful to humans according to the cytotoxicity analysis. Taking into consideration current developments in the COVID-19 pandemic, the obtained results hold a lot of promise for the design of improved protection equipment. Future research should progress to evaluation of the antiviral efficiency of ZIF-8 against actual SARS-CoV-2.

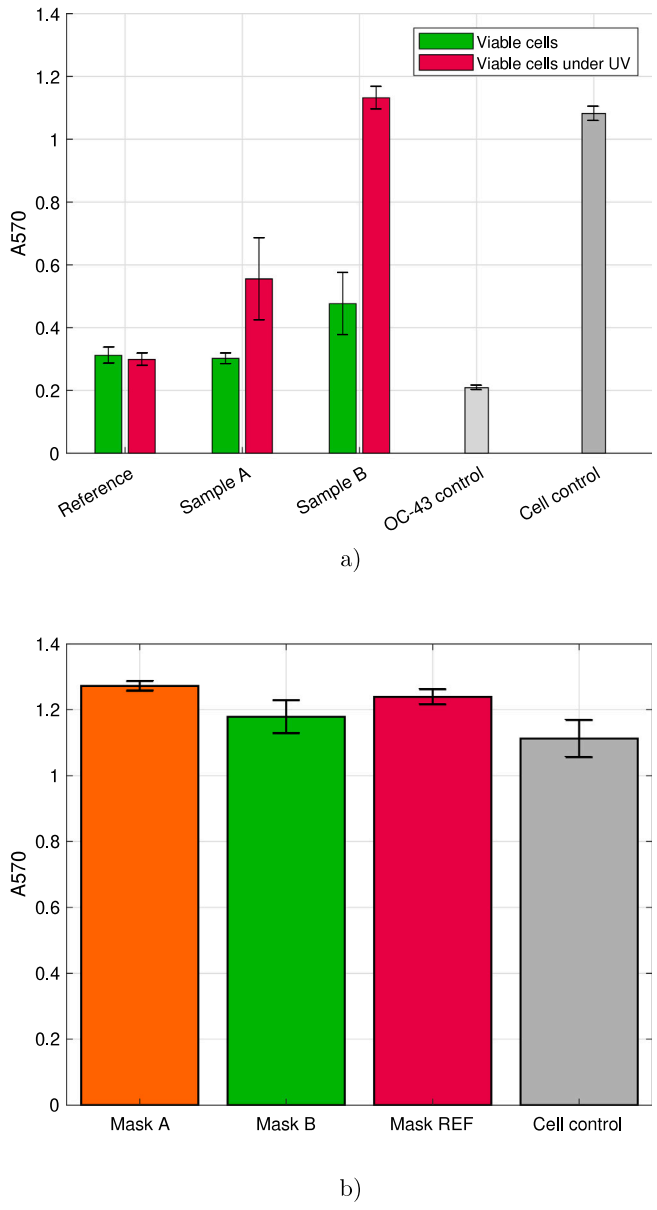

Fig. 6. Results of antiviral efficacy of ZIF-8-modified mask materials against low-pathogenic HCoV-OC43 coronavirus after 1 h of contact time: (a) mean results for the antiviral activity, (b) cytotoxicity of samples. (For interpretation of the references to color in this figure legend, the reader is referred to the web version of this article.)

CRediT authorship contribution statement

Daria Givirovskaia: Writing – original draft, Visualization, Methodology, Investigation, Formal analysis, Conceptualization. **Georgy Givirovskiy:** Conceptualization, Formal analysis, Investigation, Methodology, Visualization, Writing – original draft. **Marjo Haapakoski:** Writing – original draft, Methodology, Investigation, Formal analysis, Conceptualization, Visualization. **Sanna Hokkanen:** Conceptualization, Formal analysis, Investigation, Methodology, Visualization, Writing – original draft. **Vesa Ruuskanen:** Writing – review & editing, Supervision. **Satu Salo:** Conceptualization, Formal analysis, Investigation, Methodology, Visualization, Writing – review & editing. **Varpu Marjomäki:** Writing – review & editing, Supervision, Methodology, Conceptualization. **Jero Ahola:** Supervision, Writing – review & editing. **Eveliina Repo:** Writing – review & editing, Supervision, Resources, Project administration, Funding acquisition.

Declaration of competing interest

The authors declare that they have no known competing financial interests or personal relationships that could have appeared to influence the work reported in this paper.

Acknowledgment

The authors are grateful for support from Business Finland (Korona Co-creation, decision number 39797/31/2020) and the European Regional Development Fund (REACT-EU, Regional Council of Etelä-Karjala, project code A77605).

References

[1] Worldometer, Coronavirus update (live): Cases and deaths from COVID-19 virus pandemic, 2021, URL https://www.worldometers.info/coronavirus/.
[2] J. Howard, A. Huang, Z. Li, Z. Tufekci, V. Zdimal, An evidence review of face masks against COVID-19, Proc. Natl. Acad. Sci. USA 118 (4) (2021) 1–12, http://dx.doi.org/10.1073/pnas.2014564118.
[3] C.J. Worby, H.H. Chang, Face mask use in the general population and optimal resource allocation during the COVID-19 pandemic, Nature Commun. 11 (1) (2020) 1–9, http://dx.doi.org/10.1038/s41467-020-17922-x.
[4] WHO, Mask Use in the Context of COVID-19: Interim Guidance, Technical Documents, 2020.
[5] M. Liang, L. Gao, C. Cheng, Q. Zhou, J. Patrick, K. Heiner, C. Sun, Efficacy of face mask in preventing respiratory virus transmission : A systematic review and meta-analysis, Travel Med. Infect. Dis. 36 (2020) 101751, http://dx.doi.org/10.1016/j.tmaid.2020.101751.
[6] T. Jefferson, R. Foxlee, C.D. Mar, L. Dooley, E. Ferroni, B. Hewak, Physical interventions to interrupt or reduce the spread of respiratory viruses: systematic review, BMJ 336 (2008) 1–9, http://dx.doi.org/10.1136/bmj.39393.510347.BE.
[7] S. Feng, C. Shen, N. Xia, W. Song, M. Fan, B.J. Cowling, Rational use of face masks in the COVID-19 pandemic, Lancet Respir. Med. 8 (2020) 434–436, http://dx.doi.org/10.1016/S2213-2600(20)30134-X.
[8] J.C. Rubio-Romero, M.C. Pardo-Ferreira, J.A. Torrecilla-García, S. Calero-Castro, Disposable masks: Disinfection and sterilization for reuse, and non-certified manufacturing, in the face of shortages during the COVID-19 pandemic, Saf. Sci. 129 (2020) 1–11.
[9] M. Loeb, N. Dafoe, J. Mahony, M. John, A. Sarabia, V. Glavin, R. Webby, M. Smieja, D. Earn, S. Chong, A. Webb, S.D. Walter, Surgical mask vs N95 respirator among health care workers, JAMA 302 (17) (2009) 1865–1871.
[10] B.J. Cowling, Y. Zhou, D.K.M. Ip, G. Leung, A. Aiello, Face masks to prevent transmission of influenza virus : a systematic review, Epidemiol. Infect. (138) (2010) 449–456, http://dx.doi.org/10.1017/S0950268809991658.
[11] J. Xiao, E.Y.C. Shiu, H. Gao, J.Y. Wong, M.W. Fong, S. Ryu, B.J. Cowling, Nonpharmaceutical measures for pandemic influenza in nonhealthcare settings — Personal protective and environmental measures, Emerg. Infect. Diseases 26 (5) (2020) 967–975.
[12] R. Zhang, Y. Li, A.L. Zhang, Y. Wang, M.J. Molina, Identifying airborne transmission as the dominant route for the spread of COVID-19, Proc. Natl. Acad. Sci. USA 117 (26) (2020) 14857–14863, http://dx.doi.org/10.1073/pnas.2018637117.
[13] L. Delanghe, E. Cauwenberghs, I. Spacova, I. Boeck, I. De Boeck, W. Van Beeck, K. Pepermans, I. Claes, D. Vandenheuvel, V. Verhoeven, S. Lebeer, Cotton and surgical face masks in community settings : Bacterial contamination and face mask hygiene, Front. Med. 8 (2021) 1–12, http://dx.doi.org/10.3389/fmed.2021.732047.
[14] N.A. Hasan, B.A. Young, A.T. Minard-smith, K. Saeed, H. Li, E.M. Heizer, N.J. Mcmillan, R. Isom, A.S. Abdullah, D.M. Bornman, S.A. Faith, Y. Choi, M.L. Dickens, T.A. Cebula, R.R. Colwell, Microbial community profiling of human saliva using shotgun metagenomic sequencing, PLoS One 9 (5) (2014) e97699, http://dx.doi.org/10.1371/journal.pone.0097699.
[15] A.A. Chughtai, S. Stelzer-braid, W. Rawlinson, G. Pontivivo, Q. Wang, Y. Pan, D. Zhang, Y. Zhang, L. Li, C.R. Macintyre, Contamination by respiratory viruses on outer surface of medical masks used by hospital healthcare workers, BMC Infect. Dis. 19 (491) (2019) 1–8, http://dx.doi.org/10.1186/s12879-019-4109-x.
[16] C.B. Hiragond, A.S. Kshirsagar, V.V. Dhapte, T. Khanna, P. Joshi, P.V. More, Enhanced anti-microbial response of commercial face mask using colloidal silver nanoparticles, Vacuum 156 (2018) 475–482, http://dx.doi.org/10.1016/j.vacuum.2018.08.007.
[17] E. Sharifipour, S. Shams, M. Esmkhani, J. Khodadadi, R. Fotouhi-ardakani, Evaluation of bacterial co-infections of the respiratory tract in COVID-19 patients admitted to ICU, BMC Infect Dis. 20 (646) (2020) 1–7.
[18] R. Mirzaei, P. Goodarzi, M. Asadi, A. Soltani, S. Jalalifar, R. Mohammadzadeh, A. Teimoori, Bacterial co-infections with SARS-CoV-2, IUBMB Life 72 (10) (2020) 2097–2111, http://dx.doi.org/10.1002/iub.2356.

[19] V.K. Sharma, R.A. Yngard, Y. Lin, Silver nanoparticles : Green synthesis and their antimicrobial activities, Adv. Colloid Interface Sci. 145 (1–2) (2009) 83–96, http://dx.doi.org/10.1016/j.cis.2008.09.002.

[20] G. Ren, D. Hu, E.W.C. Cheng, M.A. Vargas-reus, P. Reip, R.P. Allaker, Characterisation of copper oxide nanoparticles for antimicrobial applications, Int. J. Antimicrob. Agents 33 (2009) 587–590, http://dx.doi.org/10.1016/j.ijantimicag.2008.12.004.

[21] J. Ramyadevi, K. Jeyasubramanian, A. Marikani, G. Rajakumar, A. Abdul, Synthesis and antimicrobial activity of copper nanoparticles, Mater. Lett. 71 (2012) 114–116, http://dx.doi.org/10.1016/j.matlet.2011.12.055.

[22] Y. Kumar, R. Adelung, C. Röhl, D. Shukla, F. Spors, V. Tiwari, Virostatic potential of micro – nano filopodia-like ZnO structures against herpes simplex virus-1, Antivir. Res. 92 (2) (2011) 305–312, http://dx.doi.org/10.1016/j.antiviral.2011.08.017.

[23] F. Martinez-Gutierrez, P.L. Olive, A. Banuelos, E. Orrantia, N. Nino, E.M. Sanchez, F. Ruiz, H. Bach, Y. Av-Gay, Synthesis , characterization , and evaluation of antimicrobial and cytotoxic effect of silver and titanium nanoparticles, Nanomed.: Nanotechnol. Biol. Med. 6 (5) (2010) 681–688, http://dx.doi.org/10.1016/j.nano.2010.02.001.

[24] S. Perni, C. Piccirillo, J. Pratten, P. Prokopovich, W. Chrzanowski, I.P. Parkin, M. Wilson, The antimicrobial properties of light-activated polymers containing methylene blue and gold nanoparticles, Biomaterials 30 (1) (2009) 89–93, http://dx.doi.org/10.1016/j.biomaterials.2008.09.020.

[25] S. Mallakpour, E. Azadi, C.M. Hussain, The latest strategies in the fight against the COVID-19 pandemic: the role of metal and metal oxide nanoparticles, New J. Chem. 45 (2021) 6167–6179, http://dx.doi.org/10.1039/D1NJ00047K.

[26] Y. Zhao, A new era of metal organic framework nanomaterials and applications, ACS Appl. Nano Mater. 3 (2020) 4917–4919, http://dx.doi.org/10.1021/acsanm.0c01241.

[27] A.E. Baumann, D.A. Burns, B. Liu, V.S. Thoi, Metal-organic framework functionalization and design strategies for advanced electrochemical energy storage devices, Commun. Chem. 2 (86) (2019) 1–14, http://dx.doi.org/10.1038/s42004-019-0184-6.

[28] S.P. Shet, S.S. Priya, K. Sudhakar, M. Tahir, A review on current trends in potential use of metal-organic framework for hydrogen storage, Int. J. Hydrog. Energy 46 (21) (2021) 11782–11803, http://dx.doi.org/10.1016/j.ijhydene.2021.01.020.

[29] L. Rani, J. Kaushal, A.L. Srivastav, P. Mahajan, A critical review on recent developments in MOF adsorbents for the elimination of toxic heavy metals from aqueous solutions, Environ. Sci. Pollut. Res. 27 (2020) 44771–44796.

[30] K. Adesina Adegoke, O. Samuel Agboola, J. Ogunmodede, A. Oluyomi Araoye, O. Solomon Bello, Metal-organic frameworks as adsorbents for sequestering organic pollutants from wastewater, Mater. Chem. Phys. 253 (2020) 123246, http://dx.doi.org/10.1016/j.matchemphys.2020.123246, URL https://www.sciencedirect.com/science/article/pii/S0254058420306167.

[31] D.K.J.A. Wanigarathna, J. Gao, B. Liu, Metal organic frameworks for adsorption-based separation of fluorocompounds: a review, Mater. Adv. 1 (2020) 310–320, http://dx.doi.org/10.1039/D0MA00083C.

[32] Z. Chu, X. Gao, C. Wang, T. Wang, G. Wang, Metal–organic frameworks as separators and electrolytes for lithium–sulfur batteries, J. Mater. Chem. A 9 (2021) 7301–7316, http://dx.doi.org/10.1039/D0TA11624F.

[33] S. Qiu, M. Xue, G. Zhu, Metal–organic framework membranes: from synthesis to separation application, Chem. Soc. Rev. 43 (2014) 6116–6140, http://dx.doi.org/10.1039/C4CS00159A.

[34] Q. Qian, P.A. Asinger, M.J. Lee, G. Han, K. Mizrahi Rodriguez, S. Lin, F.M. Benedetti, A.X. Wu, W.S. Chi, Z.P. Smith, Mof-based membranes for gas separations, Chem. Rev. 120 (16) (2020) 8161–8266, http://dx.doi.org/10.1021/acs.chemrev.0c00119, arXiv:https://doi.org/10.1021/acs.chemrev.0c00119 PMID: 32608973.

[35] W.-J. Li, M. Tu, R. Cao, R.A. Fischer, Metal–organic framework thin films: electrochemical fabrication techniques and corresponding applications & perspectives, J. Mater. Chem. A 4 (2016) 12356–12369, http://dx.doi.org/10.1039/C6TA02118B.

[36] V. Pascanu, G. González Miera, A.K. Inge, B. Martín-Matute, Metal–organic frameworks as catalysts for organic synthesis: A critical perspective, J. Am. Chem. Soc. 141 (18) (2019) 7223–7234, http://dx.doi.org/10.1021/jacs.9b00733, arXiv:https://doi.org/10.1021/jacs.9b00733 PMID: 30974060.

[37] M. Ali, E. Pervaiz, T. Noor, O. Rabi, R. Zahra, M. Yang, Recent advancements in MOF-based catalysts for applications in electrochemical and photoelectrochemical water splitting: A review, Int. J. Energy Res. 45 (2) (2021) 1190–1226, http://dx.doi.org/10.1002/er.5807, arXiv:https://onlinelibrary.wiley.com/doi/pdf/10.1002/er.5807 URL https://onlinelibrary.wiley.com/doi/abs/10.1002/er.5807.

[38] Y. Wang, Y. Hu, Q. He, J. Yan, H. Xiong, N. Wen, S. Cai, D. Peng, Y. Liu, Z. Liu, Metal-organic frameworks for virus detection, Biosens. Bioelectron. 169 (2020) 112604, http://dx.doi.org/10.1016/j.bios.2020.112604.

[39] S. Zhang, X. Pei, H. Gao, S. Chen, J. Wang, Metal-organic framework-based nanomaterials for biomedical applications, Chin. Chem. Lett. 31 (5) (2020) 1060–1070, http://dx.doi.org/10.1016/j.cclet.2019.11.036.

[40] R. Riccò, W. Liang, S. Li, J.J. Gassensmith, F. Caruso, C. Doonan, P. Falcaro, Metal–organic frameworks for cell and virus biology: A perspective, ACS Nano 12 (1) (2018) 13–23, http://dx.doi.org/10.1021/acsnano.7b08056, arXiv:https://doi.org/10.1021/acsnano.7b08056 PMID: 29309146.

[41] G.A. Udourioh, M.M. Solomon, E.I. Epelle, Metal organic frameworks as biosensing materials for COVID-19, Cell Mol. Bioeng. 6 (2021) 1–19, http://dx.doi.org/10.1007/s12195-021-00686-9.

[42] M. Almáši, A review on state of art and perspectives of metal-organic frameworks (MOFs) in the fight against coronavirus SARS-CoV-2, J. Coord. Chem. (2021) 1–17, http://dx.doi.org/10.1080/00958972.2021.1965130, arXiv:https://doi.org/10.1080/00958972.2021.1965130.

[43] H.-C. Zhou, J.R. Long, O.M. Yaghi, Introduction to metal–organic frameworks, Chem. Rev. 112 (2) (2012) 673–674, http://dx.doi.org/10.1021/cr300014x, arXiv:https://doi.org/10.1021/cr300014x PMID: 22280456.

[44] R. Li, T. Chen, X. Pan, Metal–organic-framework-based materials for antimicrobial applications, ACS Nano 15 (3) (2021) 3808–3848, http://dx.doi.org/10.1021/acsnano.0c09617, arXiv:https://doi.org/10.1021/acsnano.0c09617 PMID: 33629585.

[45] K.S. Park, Z. Ni, A.P. Côté, J.Y. Choi, R. Huang, F.J. Uribe-Romo, H.K. Chae, M. O'Keeffe, O.M. Yaghi, Exceptional chemical and thermal stability of zeolitic imidazolate frameworks, Proc. Natl. Acad. Sci. USA 103 (27) (2006) 10186–10191, http://dx.doi.org/10.1073/pnas.0602439103, arXiv:https://www.pnas.org/content/103/27/10186.full.pdf URL https://www.pnas.org/content/103/27/10186.

[46] P. Li, J. Li, X. Feng, J. Li, Y. Hao, J. Zhang, H. Wang, A. Yin, J. Zhou, X. Ma, B. Wang, Metal-organic frameworks with photocatalytic bactericidal activity for integrated air cleaning, Nature Commun. 10 (2177) (2019) 1–10, http://dx.doi.org/10.1038/s41467-019-10218-9.

[47] M. Martí, A. Tuñón Molina, F.L. Aachmann, Y. Muramoto, T. Noda, K. Takayama, A. Serrano-Aroca, Protective face mask filter capable of inactivating SARS-CoV-2, and methicillin-resistant staphylococcus aureus and staphylococcus epidermidis, Polymers 13 (2) (2021) http://dx.doi.org/10.3390/polym13020207, URL https://www.mdpi.com/2073-4360/13/2/207.

[48] K. Takayama, A. Tuñón Molina, A. Cano-Vicent, Y. Muramoto, T. Noda, J.L. Aparicio-Collado, R. Sabater i Serra, M. Martí, A. Serrano-Aroca, Non-woven infection prevention fabrics coated with biobased cranberry extracts inactivate enveloped viruses such as SARS-CoV-2 and multidrug-resistant bacteria, Int. J. Mol. Sci. 22 (23) (2021) http://dx.doi.org/10.3390/ijms222312719, URL https://www.mdpi.com/1422-0067/22/23/12719.

[49] A. Cano-Vicent, A. Tuñón Molina, M. Martí, Y. Muramoto, T. Noda, K. Takayama, A. Serrano-Aroca, Antiviral face mask functionalized with solidified hand soap: Low-cost infection prevention clothing against enveloped viruses such as SARS-CoV-2, ACS Omega 6 (36) (2021) 23495–23503, http://dx.doi.org/10.1021/acsomega.1c03511.

[50] V. Palmieri, F. De Maio, M. De Spirito, M. Papi, Face masks and nanotechnology: Keep the blue side up, Nano Today 37 (2021) 101077, http://dx.doi.org/10.1016/j.nantod.2021.101077, URL https://www.sciencedirect.com/science/article/pii/S1748013221000025.

[51] A. Tuñón Molina, K. Takayama, E.M. Redwan, V.N. Uversky, J. Andrés, A. Serrano-Aroca, Protective face masks: Current status and future trends, ACS Appl. Mater. Interfaces 13 (48) (2021) 56725–56751, http://dx.doi.org/10.1021/acsami.1c12227.

[52] J. Goscianska, R. Freund, S. Wuttke, Nanoscience versus viruses: The SARS-CoV-2 case, Adv. Funct. Mater. (2021) 2107826, http://dx.doi.org/10.1002/adfm.202107826, URL https://onlinelibrary.wiley.com/doi/abs/10.1002/adfm.202107826.

[53] N. Getachew, Y. Chebude, I. Diaz, M. Sanchez-Sanchez, Room temperature synthesis of metal organic framework MOF-2, J. Porous Mater. 21 (5) (2014) 769–773, http://dx.doi.org/10.1007/s10934-014-9823-6.

[54] J.A. Cusumano, A.C. Dupper, Y. Malik, E.M. Gavioli, J. Banga, A. Berbel Caban, D. Nadkarni, A. Obla, C.V. Vasa, D. Mazo, D.R. Altman, Staphylococcus aureus bacteremia in patients infected with COVID-19: A case series, Open Forum Infect. Dis. 7 (11) (2020) http://dx.doi.org/10.1093/ofid/ofaa518.

[55] M. Raeiszadeh, B. Adeli, A critical review on ultraviolet disinfection systems against COVID-19 outbreak: Applicability, validation, and safety considerations, ACS Photon. 7 (11) (2020) 2941–2951, http://dx.doi.org/10.1021/acsphotonics.0c01245.

[56] T.S. Fung, D.X. Liu, Similarities and dissimilarities of COVID-19 and other coronavirus diseases, Annu. Rev. Microbiol. 75 (1) (2021) 19–47, http://dx.doi.org/10.1146/annurev-micro-110520-023212, arXiv:https://doi.org/10.1146/annurev-micro-110520-023212 PMID: 33492978.

[57] A. Schejn, L. Balan, V. Falk, L. Aranda, G. Medjahdi, R. Schneider, Controlling ZIF-8 nano- and microcrystal formation and reactivity through zinc salt variations, CrystEngComm 16 (2014) 4493–4500, http://dx.doi.org/10.1039/C3CE42485E.

[58] K. Oleksii, J. Commenge, H. Alem, E. Girot, K. Mozet, G. Medjahdi, R. Schneider, Microfluidic reactors for the size-controlled synthesis of ZIF-8 crystals in aqueous phase, Mater. Des. 122 (2017) 31–41, http://dx.doi.org/10.1016/j.matdes.2017.03.002.

[59] Y. Yuan, Y. Zhang, Enhanced biomimic bactericidal surfaces by coating with positively-charged ZIF nano-dagger arrays, Nanomed.: Nanotechnol. Biol. Med. 13 (7) (2017) 2199–2207, http://dx.doi.org/10.1016/j.nano.2017.06.003, URL https://www.sciencedirect.com/science/article/pii/S1549963417301090.

[60] J.M. Belanger, Y. Raviv, M. Viard, M.J. de la Cruz, K. Nagashima, R. Blumenthal, Effects of UVA irradiation, aryl azides, and reactive oxygen species on the orthogonal inactivation of the human immunodeficiency virus (HIV-1), Virol. 417 (1) (2011) 221–228, http://dx.doi.org/10.1016/j.virol.2011.06.007, URL https://www.sciencedirect.com/science/article/pii/S0042682211002716.

[61] A.A. Abd-Elghaffar, A.E. Ali, A.A. Boseila, M.A. Amin, Inactivation of rabies virus by hydrogen peroxide, Vaccine 34 (6) (2016) 798–802, http://dx.doi.org/10.1016/j.vaccine.2015.12.041, URL https://www.sciencedirect.com/science/article/pii/S0264410X15018381.

[62] J. Dembinski, O. Hungnes, A. Germundsson, A.-C. Kristoffersen, B. Haneberg, S. Mjaaland, Hydrogen peroxide inactivation of influenza virus preserves antigenic structure and immunogenicity, J. Virol. Methods 207 (2014) 232–237, http://dx.doi.org/10.1016/j.jviromet.2014.07.003.